ChemComm

CO_2 switchable adhesion of ionic polydimethylsiloxane elastomers

Journal:	*ChemComm*
Manuscript ID	CC-COM-09-2023-004575.R1
Article Type:	Communication

COMMUNICATION

CO_2 switchable adhesion of ionic polydimethylsiloxane elastomers

Yohei Miwa, [a,b,*] Masatoshi Tsunoda,[a] Shoei Shimozaki,[a] Rina Sawada,[a] and Shoichi Kutsumizu,[a]

Received 00th January 20xx,
Accepted 00th January 20xx

DOI: 10.1039/x0xx00000x

We have develped ionic polydimethylsiloxane elastomers that rapidly and reversibly increase their adhesion upon exposure to carbon dioxide (CO_2) gas. The CO_2 molecules dissolve quickly into the ionic aggregates, physically crosslinking the polymer chains and plasticizing them. The elastomer consequently becomes softer and more adhesive upon exposure to CO_2.

On-demand tuning of the adhesion is ubiquitous in nature. For example, geckos produce adhesion in their feet to grip a surface strongly. However, they can reduce the adhesion quickly to release their feet from the surface. The quick switching of the adhesion in its feet thus allows a gecko to even walk on a wall.[1] Such quick and on-demand switch-ability of adhesion is useful for many applications, including the slip resistance of grips and the temporary fixation of products. “Switchable adhesives” that change their adhesion when subjected to various external stimuli have therefore attracted considerable interest.[2,3] Stimuli such as heat,[4–6] light,[7,8] mechanical force,[9,10] chemicals,[11,12] and moisture[13] have been applied previously to switch the adhesion of materials. In many cases, thermodynamic transitions of molecules subjected to external stimuli have been applied for this purpose. For example, De Crevoisier and Liebler et al. designed a thermo-responsive switchable adhesive in which the adhesion of a fluorinated liquid-crystal polymer changes upon heating/cooling due to the phase transition between its smectic liquid-crystalline and amorphous states.[4] Furthermore, Ohzono and Terentjev et al. recently studied the switching behaviour of adhesion in response to temperature changes in nematic liquid-crystal elastomers, and they found that switching of the adhesion is mainly due to changes in the bulk viscoelasticity.[6] On the other hand, except for very limited studies, [14,15] gases have not received much attention as triggers to increase the adhesion of materials.

Carbon dioxide (CO_2) is clean, nontoxic, non-flammable, and available at low cost because CO_2 gas is abundant in nature. Recently, many smart polymeric materials have been developed that employ CO_2 gas as a trigger to switch their properties.[16,17] In particular, Weiss et al. reported that amine-modified polydimethylsiloxane (PDMS) oil changes to a rubber-like material upon exposure to bubbling CO_2 gas.[14] In this case, the PDMS chains are crosslinked via ammonium carbamates that

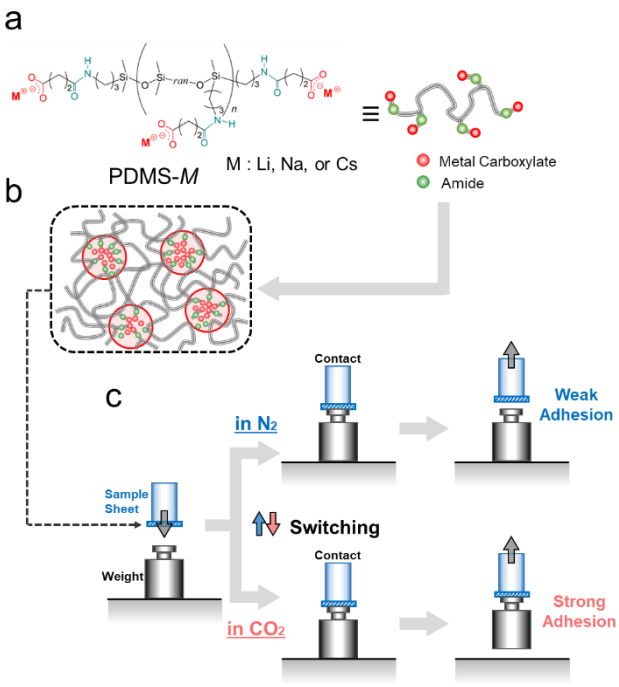

Fig. 1 (a) Chemical structure and (b) schematic illustration of the aggregated state of PDMS-*M*. (c) Overview of CO_2-responsive adhesion of PDMS-*M*. The PDMS-*M* sheet increases its adhesion in CO_2.

[a] *Department of Chemistry and Biomolecular Science, Faculty of Engineering, Gifu University, Yanagido, Gifu 501-1193, Japan. E-mail: miwa.yohei.y6@f.gifu-u.ac.jp*
[b] *PRESTO, Japan Science and Technology Agency, Kawaguchi Center Building 4-1-8, Honcho, Kawaguchi, Saitama 332-0012, Japan.*
† Electronic Supplementary Information (ESI) available: Synthesis and characterization of polymers supplementary. See DOI: 10.1039/x0xx00000x

form between the CO_2 molecules and the amine groups. These authors demonstrated that the rubber-like material adheres strongly to steel and glass plates, and they reported that the adhesive properties of this material persist for more than 24 h in air.

In the present work, we propose a new category of switchable adhesive elastomers that is quickly and reversibly responsive to CO_2 gas. The adhesion switching of these elastomers is easy to manipulate. Moreover, these elastomers do not require heat, light, electricity, or other energy to switch their adhesion. In our elastomers, a few mol% of carboxy groups—fully neutralized by the cations of lithium (Li^+), sodium (Na^+), or cesium (Cs^+)—are attached along the main chain of PDMS (Fig. 1a). The ionic groups aggregate with each other to form spherical nanosized aggregates that act as physical crosslinks (Fig. 1b). CO_2 gas plasticizes the ionic aggregates and promotes network rearrangement within the elastomer, where ionic groups hop between neighbouring aggregates.[18] As a result, the ionic PDMS elastomer is plasticized by exposure to CO_2 gas. Furthermore, we found that the adhesion of this elastomer is enhanced in the presence of CO_2 gas. For example, a sheet of the ionic PDMS elastomer neutralized with Cs^+ is adhesive in a CO_2 atmosphere and can lift a weight, while the same weight cannot be lifted in N_2 atmosphere (Fig. 1c and Video S1, ESI†). In this work, we have studied the performance of these elastomers and the mechanism responsible for their CO_2-responsive adhesion.

We note the ionic PDMS elastomers neutralized with Li^+, Na^+, or Cs^+ cations by PDMS-*M* (where *M* stands for Li, Na, or Cs). The chemical structure of PDMS-*M* is shown in Fig. 1a. The PDMS-*M* has 3.5 mol% of metal carboxylates at the chain ends and at random positions along the polymer backbone. The weight-average molecular weight of the PDMS-*M*, determined by gel-permeation chromatography with PDMS standards, is 113,000 and its polydispersity index is 5.00. We further characterized the PDMS-*M* using ^{1}H-NMR (Fig. S1, ESI†) and FT-IR (Fig. S2, ESI†).

Fig. 2a shows the CO_2 uptake of PDMS-*M* monitored via weight change. The weight increments increase in the following order: PDMS-Li < PDMS-Na < PDMS-Cs. This indicates that the main driving force for the CO_2 uptake by PDMS-*M* is the interaction between the CO_2 molecules and the metal carboxylates. We consider that CO_2 molecules interact with carboxylate anions[19] in addition to metal cations. The degree of dissociation between carboxylate anion and metal cation increases as the radius of the cation increases. This would increase the interaction between CO_2 molecules and carboxylate anions. Due to the high gas permeability of PDMS, the uptake of CO_2 occurs rapidly.[20] Even for PDMS without ionic groups, we observed a slight CO_2 absorption because PDMS is CO_2-philic.[21] The uptake of CO_2 by PDMS-Li is comparable to that of PDMS, which indicates that there is little interaction between the lithium carboxylates and the CO_2 molecules.

Fig. 2b compares the small-angle X-ray scattering patterns for PDMS-*M* measured in atmospheres of N_2 and CO_2 gas. In contrast to the absence of scattering by PDMS, PDMS-*M* exhibits a broad peak at the scattering vector $q \approx 1.1$ nm^{-1}. Here, $q = (4\pi/\lambda)\sin\theta$ where 2θ is the scattering angle. This broad scattering peak is produced by the interference between the ionic aggregates. In the present work, we have simulated the scattering pattern using a model proposed by Yarusso and Cooper (YC)[22] combined with a Lorentz function that fits the upturn at low angles. The YC model assumes that spherical ionic aggregates of radius R_1 are randomly located in the polymer matrix, with the closest approach between neighbouring ionic

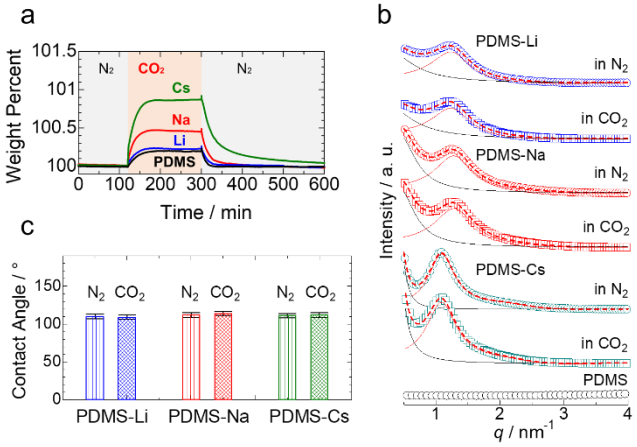

Fig. 2 Effects of CO_2 gas on (a) weight, (b) SAXS patterns, and (c) water contact angles of PDMS-*M*. In (b), the experimental scattering curves (circles) are reproduced by the YC model[22] (red solid curve) combined with a Lorentzian (black solid curve).

Table 1. Fitting parameters used for the YC model[22].

Sample	Gas	R_1 /nm	R_{CA} /nm	V_p /nm^3	ND /(10 nm)$^{-3}$	V_1 /nm^3	f_v ×10^2	f_w ×10^2
PDMS-Li	N_2	1.49	2.59	76.6	13.1	13.9	18.2	7.25
	CO_2	1.49	2.17	76.0	13.2	13.9	18.3	
PDMS-Na	N_2	1.30	2.14	68.3	14.7	9.20	13.5	7.90
	CO_2	1.32	2.12	68.8	14.5	9.63	14.0	
PDMS-Cs	N_2	1.32	2.59	94.9	10.5	9.63	10.1	12.1
	CO_2	1.44	2.60	115	8.70	12.5	10.9	

aggregates being limited to $2R_{CA}$. In this model, R_1, R_{CA}, and V_p—the average sample volume occupied by one ionic aggregate—are the parameters that determine the shape of the scattering peak. The number density ND of ionic aggregates per 1000 nm^3 is calculated from V_p. We calculated the volume of an ionic aggregate to be $V_1 = 1.33\pi R_1^3$. We also calculate the volume fraction f_v of ionic aggregates in PDMS-*M* as follows:

$$f_v = V_1 \times (ND / 1000). \quad (1)$$

The values of R_1, R_{CA}, V_1, ND, and f_v for the samples are listed in Table 1. The values of f_v for PDMS-Na and PDMS-Cs increase with exposure to CO_2 gas, while CO_2 has little effect on PDMS-Li. This result supports the fact that CO_2 molecules dissolve in the ionic aggregates in PDMS-*M*. The increments in f_v for PDMS-Li, PDMS-Na, and PDMS-Cs subjected to CO_2 gas exposure are 0%, 4 %, and 8%, respectively. This order is in good agreement with the weight increase of PDMS-*M* upon exposure to CO_2 gas, as shown in Fig. 2a.

From the viewpoint of the attractive interaction between the metal cations and CO_2 molecules, one expects Li^+ to have the strongest interaction because it has the smallest ionic radius among these metal cations. However, we observed little interaction between the Li^+ and CO_2 molecules in PDMS-Li. In addition, PDMS-Li exhibits the largest values of V_1 and f_v among the PDMS-*M*, even though the size of Li^+ is smaller than the sizes of Na^+ and Cs^+. In Table 1, we calculated the weight fraction f_w of the ionic side chain ($CH_2CH_2CH_2NHCOCH_2CH_2COOM$) in each PDMS-*M*. Interestingly, while the values of f_v is much larger than f_w for PDMS-Li, the values of f_v and f_w are relatively close to each other for PDMS-Cs. For PDMS-Na, f_v is larger than f_w, but the difference is smaller than for PDMS-Li. This implies that some PDMS backbone segments are included in the ionic aggregates in PDMS-*M*, and the number of included PDMS segments increases in the order PDMS-Cs < PDMS-Na < PDMS-Li. The inclusion of polymer segments in ionic aggregates has been reported frequently for various ionomers.[23–25] In particular, the effect of alkali-metal cations on the inclusion of polymer segments in the ionic aggregates was studied for polyisoprene (PI) ionomers, where PI was modified with carboxy groups neutralized with Li^+, Na^+, or Cs^+.[25] The inclusion of PI segments in the ionic aggregates increased in the order $Cs^+ < Na^+ < Li^+$ because of the cation–π interactions between the alkali-metal cations and the double bonds in the PI segments. For PDMS-Li, we speculate that the PDMS segments are included in the ionic aggregate due to the strong attractive interactions between the Li^+ ions and the negatively charged oxygens in the PDMS segments, thereby disturbing the interactions between Li^+ and the CO_2 molecules. It is similarly well known that Li^+ interacts attractively and strongly with the negatively charged oxygens in poly(ethylene oxide).[26]

We determined the effect of CO_2 gas on the state of the surface of PDMS-*M* using static contact-angle measurements. Fig. 2c compares the values of water contact angles for PDMS-*M* in atmospheres of N_2 and of CO_2 gas. The value of the contact angle is approximately 110°, irrespective of the type of neutralizing metal cation or gas atmosphere. This contact angle

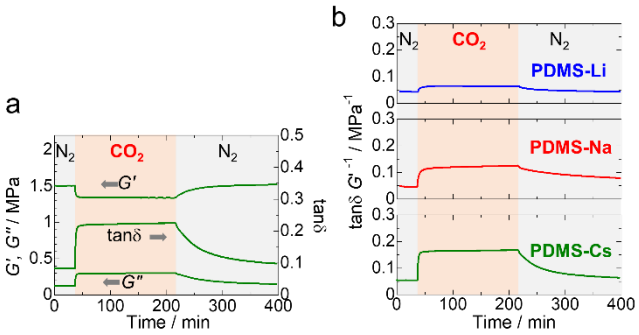

Fig. 3 (a) Effect of CO_2 gas on the viscoelastic properties of PDMS-Cs. The temperature is 25 °C, and the frequency is 1 Hz. (b) Plots of tanδ G'^{-1} for PDMS-*M* during gas switching.

also is in good agreement with that of PDMS.[27] This result indicates that the surface of PDMS-*M* is covered by PDMS segments that have small surface free energies and that the surface of PDMS-*M* is insensitive to CO_2 gas.

The effects of CO_2 gas on the storage modulus (G'), loss modulus (G''), and loss tangent (tanδ = $G''G'^{-1}$) of PDMS-Cs measured at 25°C and 1 Hz are shown in Fig. 3a. The data for PDMS-Li and PDMS-Na are shown in Fig. S3, ESI†. The parameters G'' and tanδ increase quickly upon exposure to CO_2 gas, while G' decreases due to the CO_2-induced plasticization of the specimen. On the other hand, the return of the viscoelastic values is relatively slow because of the slow release of CO_2 from the specimen. The quantity tanδ G'^{-1}, which is the practical scaling factor[6,28] employed to determine the performance of pressure-sensitive adhesives, is shown in Fig. 3b. The value of tanδ G'^{-1} increases upon exposure to CO_2 gas in the order PDMS-Li < PDMS-Na < PDMS-Cs. This trend is in good agreement with that for the CO_2 uptake of these samples shown in Fig. 2a. This result demonstrates that the dissolving of CO_2 into the ionic aggregates, which act as physical crosslinks, causes the CO_2-induced plasticization of the ionic PDMS elastomers as discussed in our previous paper.[18]

In addition, CO_2 gas significantly enhances the adhesion of the elastomers. As shown in Fig. 4a, we determined the adhesions of sample sheets using probe-tack tests at 25°C under controlled gas conditions. We placed a stainless-steel probe with a diameter of 4 mm in contact with the sample sheet at 0.5 N for 30 s and then removed the probe from the sample at a rate of 10 μm s^{-1} (Fig. 4b). We recorded the maximum force attained during the removal as the adhesion force F_{ad}. During each measurement, we switched the gas flow in the following order: $N_2 \rightarrow CO_2 \rightarrow N_2$. The adhesion behaviour of PDMS-Cs under these different gas atmospheres is shown in Fig. 4c. The data for PDMS-Li and PDMS-Na are shown in Fig. S4, ESI†. We obtained the gas dependence of the stress at adhesion from F_{ad} divided by the contact area of the probe, as shown in Fig. 4d. For PDMS-Na and PDMS-Cs, the adhesion increased quickly and significantly upon exposure to CO_2 gas, while only a slight change occurred for PDMS-Li. In particular, the adhesion of PDMS-Cs in CO_2 increases to become more than double its value in N_2. On the other hand, the return of the adhesion from its value in CO_2 to that in N_2 is relatively slow, as is also the case for

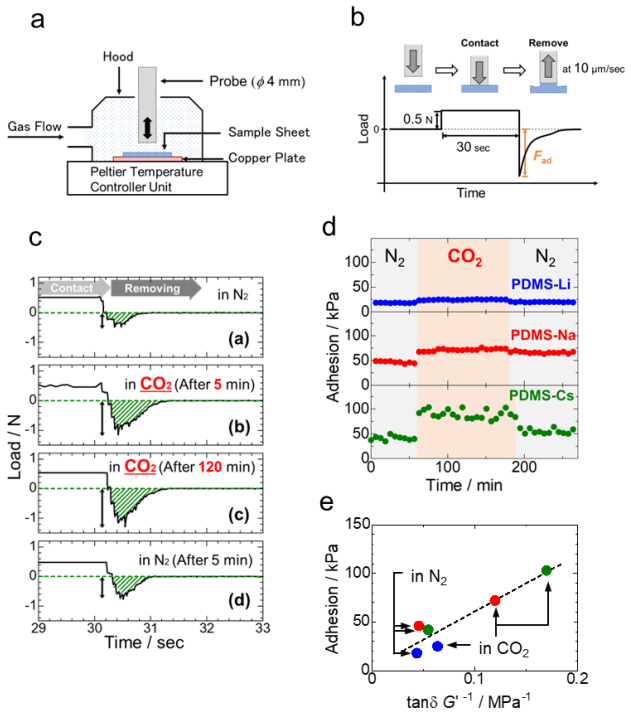

Fig. 4 Schematic illustrations of (a) gas-controlled probe-tack test and (b) conditions for adhesion measurements. (c) Selected force-vs.-time curves for PDMS-Cs at 25°C in different gases. (d) Effect of CO_2 gas on the adhesion of PDMS-*M*. (e) Plots of the adhesion of PDMS-Li (blue), PDMS-Na (red), and PDMS-Cs (green) against tanδ G'^{-1}.

the viscoelastic behaviour. As shown in Fig. 4e, we found that the adhesion of our elastomers is correlated with their tanδ G'^{-1} values. In addition, the adhesion of PDMS-Cs increases with an increase in the velocity of the probe during removal (Fig. S5, ESI†). These results demonstrate that the increase in the adhesion of our elastomers is related to their viscoelastic properties, which enhance the energy dissipation during the detachment process. On the other hand, the contact-angle measurements demonstrate that the elastomer surface is insensitive to CO_2 gas (Fig. 2a).

In summary, we have developed ionic PDMS elastomers that rapidly and reversibly increase their adhesion in the presence of CO_2 gas. These elastomers are physically crosslinked via aggregations of ionic side groups neutralized by Li^+, Na^+, or Cs^+. Under exposure to CO_2, the CO_2 molecules quickly dissolve into the ionic aggregates and plasticize them, causing the elastomer to become softer and more adhesive. In contrast, the water contact angle is insensitive to CO_2 gas. The effect of CO_2 on the structure, viscoelasticity, and adhesion of PDMS-*M* is more pronounced for PDMS-Cs, while there is little effect for PDMS-Li. For PDMS-Cs, the adhesion becomes more than double its value in N_2 to that in CO_2. In conclusion, the CO_2-responsive adhesion of the ionic PDMS elastomers is mainly caused by the change in their viscoelastic properties upon exposure to CO_2 gas.

Beam-time at PF-KEK provided by Programs 2019G116, 2020G610, and 2021G573 is acknowledged herein. This research was financially supported by the JSPS KAKENHI Grant Numbers 19K05612 (YM) and 22H02141 (YM); JST, PRESTO Grant Number JPMJPR199B (YM), Japan.

Conflicts of interest

There are no conflicts to declare.

References

1 Y. Tian, N. Pesika, H. Zeng, K. Rosenberg, B. Zhao, P. McGuiggan, K. Autumn and J. Israelachvili, *Proc. Natl. Acad. Sci.*, 2006, **103**, 19320–19325.
2 M. Kamperman and A. Synytska, *J. Mater. Chem.*, 2012, **22**, 19390–19401.
3 A. B. Croll, N. Hosseini and M. D. Bartlett, *Adv. Mater. Technol.*, 2019, **4**, 1900193.
4 G. B. Crevoisier, P. Fabre, J. M. Corpart and L. Leibler, *Science*, 1999, **285**, 1246–1249.
5 S. Reddy, E. Arzt and A. del Campo, *Adv. Mater.*, 2007, **19**, 3833–3837.
6 T. Ohzono, M. O. Saed and E. M. Terentjev, *Adv. Mater.*, 2019, **31**, 1902642.
7 H. Akiyama and M. Yoshida, *Adv. Mater.*, 2012, **24**, 2353–2356.
8 Y. Gao, K. Wu and Z. Suo, *Adv. Mater.*, 2019, **31**, 1806948.
9 P.-C. Lin, S. Vajpayee, A. Jagota, C.-Y. Huid and S. Yang, *Soft Matter*, 2008, **4**, 1830–1835.
10 T. Ohzono and K. Teraoka, *Soft Matter*, 2017, **13**, 9082–9086.
11 R. La Spina, M. R. Tomlinson, L. Ruiz-Pérez, A. Chiche, S. Langridge and M. Geoghegan, *Angew. Chem. Int. Ed.*, 2007, **46**, 6460–6463.
12 T. Nakamura, Y. Takashima, A. Hashidzume, H. Yamaguchi and A. Harada, *Nat. Commun.*, 2015, **5**, 4622.
13 M. Hara, Y. Iijima, S. Nagano and T. Seki, *Sci. Rep.*, 2021, **11**, 17683.
14 T. Yu, K. Wakuda, D. L. Blair and R. G. Weiss, *J. Phys. Chem. C*, 2009, **113**, 11546–11553.
15 Y. Li, S.Wang, H. Wu, R. Guo, Y. Liu, Z. Jiang, Z. Tian, P. Zhang, X. Cao, and B. Wang, *ACS Appl. Mater. Interfaces*, 2014, **6**, 6654–6663.
16 H. Liu, S. Lin, Y. Feng and P. Theato, *Polym. Chem.*, 2017, **8**, 12–23.
17 M. F. Cunningham and P. G. Jessop, *Macromolecules*, 2019, **52**, 6801–6816.
18 Y. Miwa, K. Taira, J. Kurachi, T. Udagawa and S. Kutsumizu, *Nat. Commun.*, 2019, **10**, 1828.
19 W. Harb, F. Ingrosso and M. F. Ruiz-López, *Theoret. Chem. Acc.* 2019, **138**, 85.
20 A. C. M. Kuo, in *Polymer Data Handbook*, (Ed. J. E. Mark), Oxford University Press, New York, 1999, 411.
21 W. Shi, N. S. Siefert and B. D. Morreale, *J. Phys. Chem. C*, 2015, **119**, 19253–19265.
22 D. J. Yarusso and S. L. Cooper, *Polymer*, 1985, **26**, 371–378.
23 S. Kutsumizu, K. Tadano, Y. Matsuda, M. Goto, H. Tachino, H. Hara, E. Hirasawa, H. Tagawa, Y. Muroga and S. Yano, *Macromolecules*, 2000, **33**, 9044–9053.
24 N. C. Zhou, C. D. Chan and K. I. Winey, *Macromolecules*, 2008, **41**, 6134–6140.
25 Y. Miwa, K. Hasegawa, T. Udagawa, Y. Shinke, S. Kutsumizu, *Phys. Chem. Chem. Phys.*, 2022, **24**, 17042–17049.
26 L. T. Costa, B. Sun, F. Jeschull and D. Brandell, *J. Chem. Phys.*, 2015, **143**, 024904.
27 H. T. Kim and O. C. Jeong, *Microelectron. Eng.*, 2011, **88**, 2281–2285.
28 T. Wang, C.-H. Lei, A. B. Dalton, C. Creton, Y. Lin, K. A. S. Fernando, Y.-P. Sun, M. Manea, J. M. Asua and J. L. Keddie, *Adv. Mater.*, 2006, **18**, 2730–2734.